Proceedings World Geothermal Congress 2005
Antalya, Turkey, 24-29 April 2005

Naphthalene Disulfonate Tracer Test Data In The Mahanagdong Geothermal Field, Leyte, Philippines

Edwin B. Herras, Farrell L. Siega and Medardo C. Magdadaro

PNOC-Energy Development Corporation, Merritt Road, Ft. Bonifacio, Taguig, Philippines

lgpf_geoservices@energy.com.ph

Keywords: Tracers, Mahanagdong, fluid flow paths

ABSTRACT

Tracer test was conducted in Mahanagdong using three types of Naphthalene Disulfonate (NDS) tracers: 1,5-NDS, 1,6-NDS and 2,6-NDS. The objective of the test is to define hydrological flow paths of cooler peripheral and injected fluids into the production sector and their assess impact to the producing wells in terms of degree of fluid mixing and cooling effect using the TRINV/ICEBOX software (United Nations University Training Programme, 1994)).

The tracers were injected simultaneously at: 1) MG4DA, close to the source of a natural groundwater recharge; 2) MG21D, located at the northwest section of the field utilized for hot brine injection; and 3) MG5RD, located at the southeast section of the field utilized for hot brine injection. Multiple tracers analyzed in a single sample but yielding discrete results can be used in evaluating several reservoir processes occurring together in a single field.

The 1,5-NDS tracer injected at MG21D indicated fast returns of injected brine into most of the wells north of the field with average velocities of 40 to 100 m/day and tracer recoveries of 0.30 to 2.0%. The conduits of the injected brine are the Malitbog, North Mamban and Ewex faults, which are the major structures intersected by MG21D and the adjacent producing wells. On the other hand, the 2,6-NDS tracer injected at MG5RD yielded positive returns in wells located south of the production field with the Lower Mahanagdong fault as conduit. The result suggests a much slower return of injected brine (ave. velocities ~ 13-17 m/day) into the production sector and tracer mass recoveries of 3 to 7%. Consistent with the result of the geochemical evaluation wherein no thermal decline was observed even though most of the wells have already shown significant increase in fluid mineralization, low brine return velocities may allow sufficient fluid heat-up. The 1,6-NDS injected at MG4DA likewise yielded positive returns in wells located at the northern section of the field, with average velocities of 7.0 to 9.0 m/day. This basically confirmed the natural groundwater recharge from the Paril area in the west, with preferential flow towards pad MGDL, the area with the highest drawdown.

Except for groundwater recharge, cooling predictions based on ICEBOX software indicate reservoir temperature decline of 0.5 to 2.0°C and 2.0 to 8.0°C in the north and south sections of the field, respectively.

1. INTRODUCTION

The Mahanagdong geothermal field, covering an area of about 10 km^2, lies within a large geothermal reservation in the island of Leyte in the central part of the Philippines (Fig. 1). It is about 7-8 kilometers south east of the Tongonan geothermal field. Both fields are collectively termed as the Greater Tongonan Geothermal field and have been explored and operated by the Philippine National Oil Company-Energy Development Corporation (PNOC-EDC) since the 1970's. These fields are two separate geothermal systems with distinct heat sources and their own convection systems. A cold and impermeable barrier, called the Mamban block separates them.

The Mahanagdong stratigraphy consists of a metamorphic basement, a conglomerate complex, an impermeable claystone unit and young andesitic lavas and pyroclastics believed to be deposited since Miocene. Structures related to the Philippine Fault provide channels for fluid movements in the field.

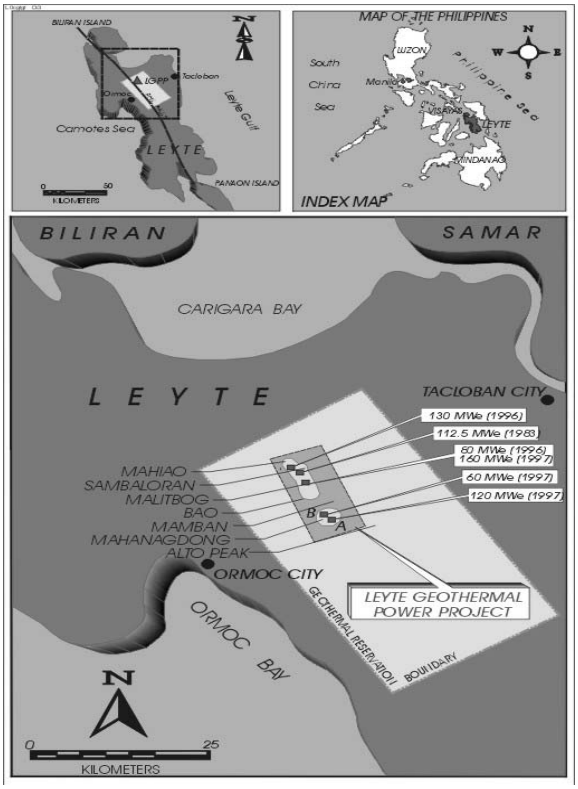

Figure 1. Location map of Mahanagdong geothermal field on Leyte Island in the central part of the Philippines.

The chemical and physical characteristics of the wells in Mahanagdong before commercial operations began in 1997 indicate that the center of the Mahanagdong geothermal system is beneath wells MG-3D and MG-14D. The temperature of the parent fluid is above 290°C and reservoir chloride of around 4000 to 4200 mg/kg. The parent fluid has high CO_2 of more than 400 mmol/100 mol water and enriched water isotopes of more than -1.0 ‰ $\delta^{18}O$.

North of the Mamban fault, the fluids are acidic with high levels of SO_4 in the liquid and high H_2S in the vapor. Reservoir chloride ranges from 3000 to 4000 mg/kg and CO_2 ranges from 200 to 400 mmol/100 mol H_2O. These fluids have temperatures of 260 to 280°C and have slightly depleted $\delta^{18}O$ that ranges from -3.0 to -2.0‰. The presence of high amounts of Mg in these fluids indicates that the fluids have not yet attained full equilibrium with the reservoir rocks.

South of the Mamban fault, the fluids have alkaline to neutral pH levels. They have temperatures of 260 to 280°C and reservoir chloride of 2500 to 300 mg/kg. The CO_2 level in this area is below 200 mmol/100 mol water while the CO_2/H_2S ratios are high as 100, indicating low levels of H_2S in the vapor phase. The fluids have slightly depleted $\delta^{18}O$ ranging from -3.0 to -2.0‰. The fluids in this sector are also found to be saturated with calcite and may possibly induce calcite blockage upon flashing inside the well bore.

The western wells, having temperatures of less than 240°C, are the coolest among the production wells. They also discharged the most diluted fluids, with less than 2500 mg/kg reservoir chloride, and are most isotopically depleted waters with less than -3.0 ‰ $\delta^{18}O$. They also have low CO_2 and H_2S contents. These values indicate the presence of a cooler type of fluid in the western part of the field.

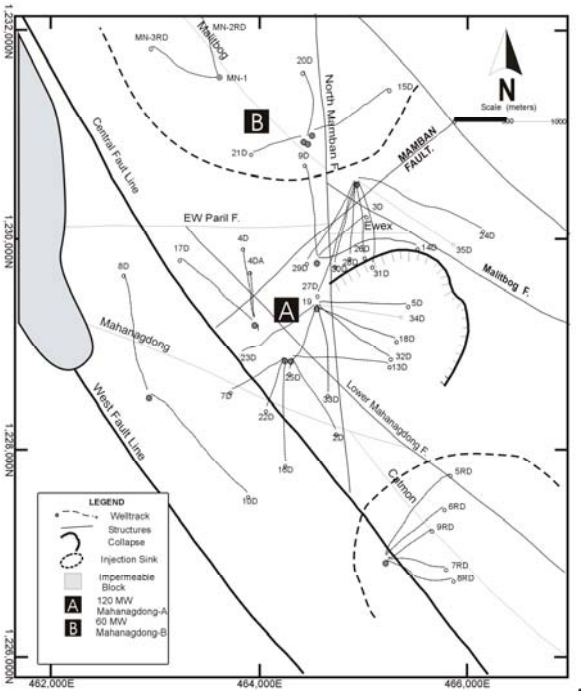

Figure 2. Development scheme of Mahanagdong field. The Mahanagdong-B (60 MW) power plant in the north and MG-A power plant (120MW) in the south, separated by a topographic low.

The Mahanagdong field was developed by dividing the area into two sectors using a topographic low related to the Mamban Fault. The Mahanagdong-A (MG-A) sector hosts a 120 MWe main plant and a 12 MWe topping cycle plant supplied by steam from 14 production wells drilled in the dominantly hot, neutral pH area in the southern part of the steam field (Fig. 2). The Mahanagdong-B (MG-B) sector, with 7 wells in the central part of the field, supplies a 60 MWe main plant and a 6 MWe topping cycle plant. The separated brine from both fields is injected back into the injection sinks located in the northern and southern parts of the field. The northern injection sink consists of five injection wells, including the acidic wells MG-15D, 20D and 21D. The southern injection sink consist of five injection wells, having a total injection capacity of 700 kg/s brine. In both injection sinks, the practice is to inject waste fluids with a temperature of 160°C.

MG-A's commercial operation began in July 1997 with more than 270 kg/s (900 t/h) of steam available at the wellheads, more than enough to supply the main plant. Meanwhile, more than 130 kg/s (468 t/h) was available for the MG-B main plant. Fig.3 shows the history of monthly mass extraction and injection in the Mahanagdong field from 1997 to 2003. The total fluid extracted at MG-A started initially at 1,000,000 tons per month while MG-B started at about 500,000 tons per month. The rate of mass extraction gradually increased to 1,750,000 and 1,000,000 tons per month in 1998, corresponding to the time when the power plants of sectors A and B of Mahanagdong began operating full-load. The rate of mass extraction in MG-A gradually increased to 2,000,000 tons per month and is maintained to the present while the extraction rate at MG-B of 1,000,000 tons per month remained continuous to the present. As a consequence of the extraction, a pressure decline of as much as 5 MPa occurred in the central part of the production field. The decline was most rapid within the limited production area of MG-B where closely spaced wells were drilled. The pressure situation across the field is bowl-like in configuration with a large depressurized central area and is over-pressured in the peripheral parts, especially in the injection sinks.

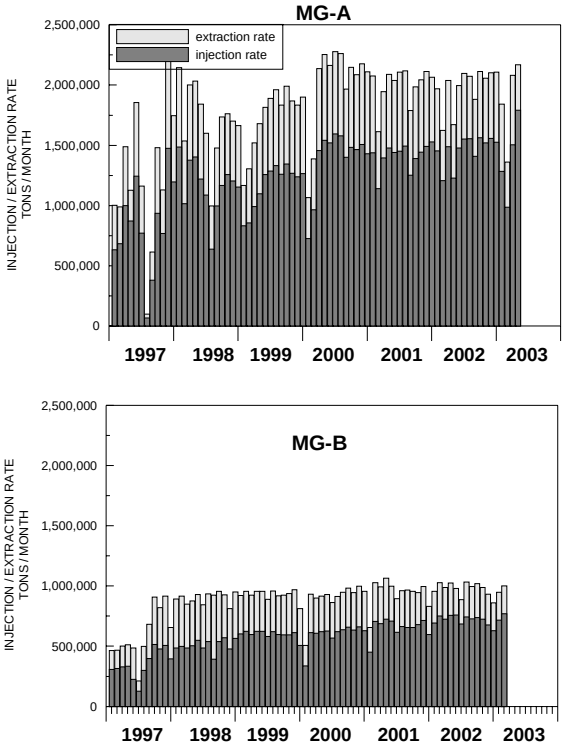

Figure 3. Plot of the monthly extraction and injection rate in the Mahanagdong field.

The initial response of the production wells to the decline in pressure and drawdown of the water level was boiling as demonstrated by wells MG-30D and MG-32D where the discharge enthalpy increased. However, this was short-lived, lasting for about 1 to 2 years only, after which the enthalpy generally returned to its baseline level.

The succeeding years was marked by a reversal in the hydrological flow path of the Mahanagdong field. The

depressurized central part of the field invited inflow of fluids from the over-pressured peripheral areas through the permeable structures summarized in Fig 4. This reversal in flow direction posed many problems in sustaining the level of steam production in the Mahanagdong field, as well as changes in the characteristics of the production wells.

Injection returns were observed to be invading the southwestern area of the field from the last quarter of 1999. High chloride, low gas fluids were noted in MG-7D, MG-16D and MG-22D. Based on chemical and structural examination, it was postulated that the injected fluids originate from the southern injection sink. Similarly, in Mahanagdong-B, signs of injection returns were also noted from the last quarter of 1999. Wells MG-26D, 28D, 30D and 31D showed an increase in field chloride and a decline in total discharge CO_2. A decline in quartz geothermometer values was observed in some of these wells. There was a general increase in field chloride concentration, represented by deep wells MG-30D and MG-31D and initially from 3600 to 3900, to 4100 to 4500 mg/kg. Such an increase in is the effect of brine injection at the northern injection sink, which has a chloride content of about 4700 mg/kg. The same fluids encroaching Mahanagdong-B wells eventually affected neighboring wells in Mahanagdong-A, namely MG-3D and MG-14D. Among the injection wells in the north, MG-21D was postulated to be the specific source of the injected fluids due to its direct structural connection with the affected production wells.

By 2001, wells MG-l, MG-23D, MG-27D and MG-29D have shown clear indications of groundwater inflow.

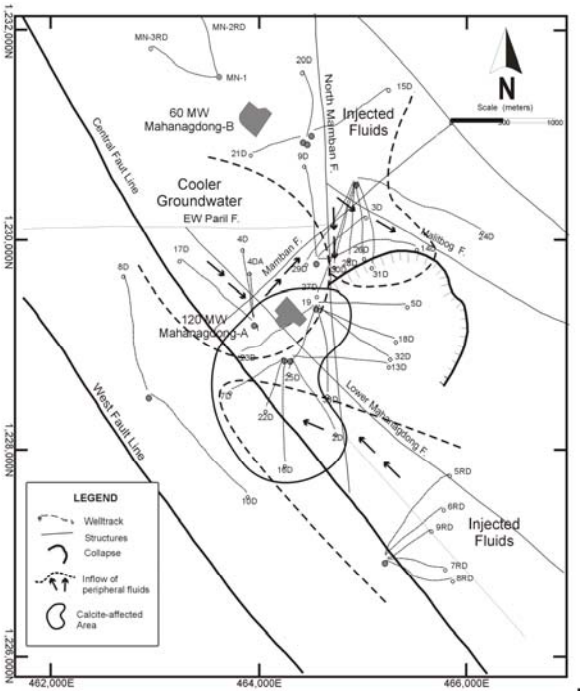

Figure 4. The present fluid flow across the field.

The compounding effects of the inflowing peripheral fluids in the Mahanagdong field have been deleterious to the steam supply. The total steam available from the Mahanagdong field was reduced by about 30% from its original capacity. However, because of a contract with the power plant operators, downsizing of electricity generation cannot be simply implemented. An important step in dealing with the situation is to identify the injection wells influencing the inflow of the unwanted cooler fluids, as well as the conduit of these fluids. It was also important to quantify the extent and rate of cold-water invasion in the production wells so that appropriate mitigation measures can be effected. This was the rationale for the Naphthalene Disulfonate (NDS) tracer study conducted in Mahanagdong beginning in January 2003.

2. NDS TRACER TESTS

Naphthalene disulfonate tracers were chosen since they have been proven to be useful as geothermal tracers, being thermally stable, environmentally benign, quite detectable by fluorescence spectroscopy and affordable. In a recent laboratory study, NDS tracers showed no decay when exposed to simulated hydrothermal conditions for one week at 330°C. These tracers were successfully tested in a field study at the Dixie Valley, Nevada geothermal reservoir (Rose et al, 2001).

The injection of NDS tracers was conducted in Mahanagdong from January 13-15, 2003. Three different types of NDS tracers were injected separately in wells MG-21D (MG-B3 pad), MG-4DA and MG-5RD (MG-RD1B pad). MG-21D is one of the acid wells drilled in the northern section of the field and is currently used as injection well for MG-B. Well MG-4DA is a production well drilled in the western part of the field, but because of substantial inflow of cooler waters into the well, the well became unfit for production. MG-5RD is one of the injection wells at MG-RD1B pad utilized for the brine disposal of MG-A.

After taking into account the reservoir thickness, porosity, resource area of the Mahanagdong area and a detection limit of ~0.9 ppb, 600 kg of 1,5 NDS was injected in MG-21D, 600 kg of 1,6-NDS in MG-4DA and 600 kg 2,6-NDS in MG-5RD. The tracers, which came in powder form, was dumped into a slurry mixer of a cementing unit and mixed with fresh water until a dissolution ratio of 300 l water to 50 kg tracer was achieved. The tracer slurry solution was then injected into the well through the wing valve in the shortest possible time to simulate instantaneous tracer slug flow in the reservoir. Prior to the tracer injection, water samples were collected from each of the monitoring stations for analysis of sulfonate baseline levels. After tracer injection, 500-ml water samples pre-treated with 5 ml of 10% HCl were collected from each station throughout the monitoring period. Water samples from the two-phase lines of the monitor wells were collected using individual ⅜-inch stainless steel cooling coils connected to the bottom sampling point. The cooling coil was immersed in half steel or plastic drums filled with water to ensure that the temperature of the sample was below 35°C. In the collection of samples from each well, the opening of the sampling valve was kept constant. 19 production wells in Mahanagdong were monitored for possible tracer returns. Water samples were collected from these wells at least twice a week and scanned for the three types of sulfonates using High Performance Liquid Chromatography (HPLC).

3.0 THEORY

The first step in analyzing tracer test data involves estimating the mass of tracer recovered from the monitor wells throughout the test. This is done on the basis of the following equation

$$mi(t) = \int_0^t Ci(s)Qi(s)ds \qquad (1)$$

where mi(t) indicates the cumulative mass recovered in production well number i as a function of time, Ci is the

tracer concentration and Qi the production rate of the well. Integration is done using TRMASS (Arason, 1993) in the ICEBOX package (United Nations University Geothermal Training Programme, 1994).

A simple one-dimensional flow-channel tracer transport model is used in simulating return data from tracer tests (Axelsson et al., 1995). It assumes that the flow between injection and production wells may be approximated by one-dimensional flow in flow-channels. These flow-channels may be parts of near-vertical fracture-zones or parts of horizontal interbeds or layers. In some cases, more than one channel may be assumed to connect an injection and production well; for example, connecting different feed-zones in the wells involved.

Flow in one dimension is given by

$$D\frac{\partial^2 C}{\partial x^2} = u\frac{\partial C}{\partial x} + \frac{\partial C}{\partial t} \qquad (2)$$

Where D is the dispersion coefficient, C the tracer concentration in the flow-channel, x the distance along the flow channel and u is the average fluid velocity in the channel given by $q/\rho A\phi$, with q the injection rate, ρ the water density, A the average cross-sectional area of the flow channel and ϕ the flow channel porosity. Molecular diffusion is neglected in this study. Assuming instantaneous injection of a mass M of tracer at time t = 0 the solution is given by:

$$c(t) = \frac{uM}{Q}\frac{1}{2\sqrt{\Pi Dt}}e^{-(x-ut)^2/4Dt} \qquad (3)$$

Here c(t) is the tracer concentration in the production well fluid, Q the production rate and x the distance between the wells involved. Conservation of the tracer according to c·Q = C·q has been assumed. The tracer interpretation software TRINV in the ICEBOX package is used for this interpretation.

The ultimate goal of tracer testing is to predict thermal breakthrough and temperature decline during long-term injection. These changes are dependent on the properties of the flow-channel, but the flow-path volume does not uniquely determine them. Cooling mainly depends on the surface area and porosity of the flow-channel. The program TRCOOL, which was used for these predictions, incorporates the following equation:

$$T(t) = T_0 - \frac{q}{Q}(T_0 - T_1)\left[1 - erf\left\{\frac{kxh}{c_w q\sqrt{K(t-x/\beta)}}\right\}\right] \qquad (4)$$

with T(t) the production fluid temperature, To the undisturbed reservoir temperature, Ti the injection temperature, q and Q the rates of injection and production, respectively, erf, the error-function, k the thermal conductivity of the reservoir rock, K its' thermal diffusivity, x the distance between injection and production wells and

$$\beta = \frac{qc_w}{\left(\langle\rho c\rangle_f hb\right)} \qquad (5)$$

with

$$\langle\rho c\rangle_f = \rho_w c_w\phi + \rho_r c_r(1-\phi) \qquad (6)$$

the volumetric heat capacity of the material in the flow-channel. ρ=density, c = heat capacity, and the indices w for water and r for rock.

To deal with the uncertainty in calculating cooling predictions on the basis of tracer test data alone, the predictions were calculated assuming that the flow-channel dimension and its physical property consisted of a high porosity, small surface area and pipe-like flow channel. This is the case where the width and height of flow channel is equal, which is the most pessimistic scenario resulting in rapid cooling.

4.0 RESULTS AND DISCUSSION

A total of 13 of the 19 (68%) production wells monitored for almost a year showed positive responses from the different tracers, confirming the influence of the peripheral waters. Summarized in Table 1 below are the production wells that indicated positive response with the corresponding tracer.

Table 1. Summary of NDS tracer positive wells.

Injection Well (Tracer)	Production wells with positive tracer response
MG21D (1,5-NDS)	MG3D, MG14D, MG28D, MG30D, MG31D
MG4DA (1,6-NDS)	MG26D, MG27D, MG29D, MG30D, MG31D
MG5RD (2,6-NDS)	MG2D, MG7D, MG16D, MG22D, MG23D

The completed breakthrough curves were processed using the *ICEBOX* software package, which include tracer test analysis, inversion of tracer test data and cooling prediction of production wells.

4.1 Transit time and Tracer Recovery

The 1,5 NDS tracer injected at MG-21D that would mimic injected brine from MG-B3 pad yielded positive responses from five wells (MG-3D, MG-14D, MG-28D, MG-30D, MG-31D) drilled in the north and in MG-DL pad. The recovery profiles show sharp breakthrough curves that indicate high velocities and low dispersion, implying an almost direct flow path of the fluids to the affected wells. These fluids reached the production wells relatively fast, ranging from 2 to 11 days from the day of injection, or equivalent to an average velocity of 1300 to 3100 m/month. The model parameters used to simulate NDS recovery suggest that these fluids passed through two flow-channels for each well pair (MG-21D versus each well) as shown in Fig. 5 and in Table 2. The results indicate that in MG-3D, for example, the calculated total mass recovery of tracer from the two flow-channels is 0.0174. The total tracer mass recovery from the 1,5-NDS affected wells is 0.0376 or 23 kg out of the 600 kg of tracer injected. The identified conduits of these fluids from MG-21D are the Malitbog Fault and Ewex faults, which are the major structures intersected by MG-3D, MG-14D and pad MGDL wells. Tracer return concentration at well MG-3D is highest, it being the nearest well to MG-21D.

The 1,6 NDS tracer injected in MG-4DA that would represent inflowing groundwater from the Paril sector indicated positive responses in wells from the north and the MG-DL wells (MG-3D, MG-14D, MG-27D, MG-29D, MG-30D and MG-31D), almost similar to the 1,5 NDS responding wells. The tracer return profiles of these wells

indicate a slow-moving fluid from MG-4DA undergoing higher dispersion and diffusion throughout the reservoir volume. These fluids reached the production wells only after 56 to 114 days from the injection day, or an average velocity of 130 to 225 m/month. The tracer was first detected in well MG-29D after 56 days, followed by MG-30D after 75 days.

Table 2. Model parameters used to simulate 1,5-NDS recovery of wells from MG-21D, where u = mean flow velocity; A = cross-sectional area; ϕ = porosity; α_L = longitudinal dispersivity of flow-channel; Mi = calculated mass recovery of tracer until infinite time; M = total mass of tracer

Well	Channel length, x (m)	u (m/s)	Aϕ (m^2)	αL (m)	Mi/M (kg/kg)
MG-3D	1100	0.0011	0.368	24	0.0031
	1200	0.00071	0.225	319	0.0143
MG-14D	1300	0.00053	0.205	9	0.0011
	1500	0.00053	0.499	335	0.0027
MG-28D	1100	0.0012	0.129	89	0.0016
	1200	0.00059	0.192	291	0.0011
MG-31D	1400	0.00071	0.646	155	0.0047
	1500	0.00025	0.221	20	0.0006
MG-30D	1100	0.00073	1.03	215	0.0077
	1200	0.00019	0.343	15	0.00068

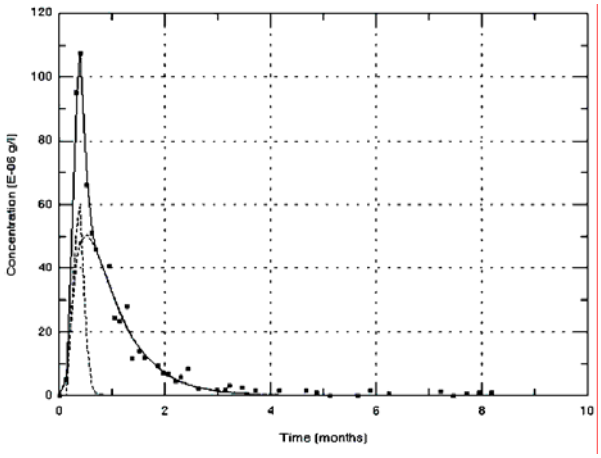

Figure 5. Observed and simulated 1,5-NDS tracer recovery in well MG-3D

Table 3. Model parameters used to simulate 1,6-NDS recovery of wells from MG-4DA.

Well	Channel length, x (m)	u (m/s)	Aϕ (m^2)	αL (m)	Mi/M (kg/kg)
MG29D	1100	0.000069	5.28	58	0.0357
MG3D	1200	0.000050	1.11	139	0.0054
MG27D	1300	0.000068	7.11	77	0.0471
MG30D	1100	0.000057	12.28	92	0.0677
MG31D	1400	0.000071	4.47	85	0.0306
MG14D	1400	0.000061	0.224	9	0.0013
	1500	0.000087	0.222	47	0.0019

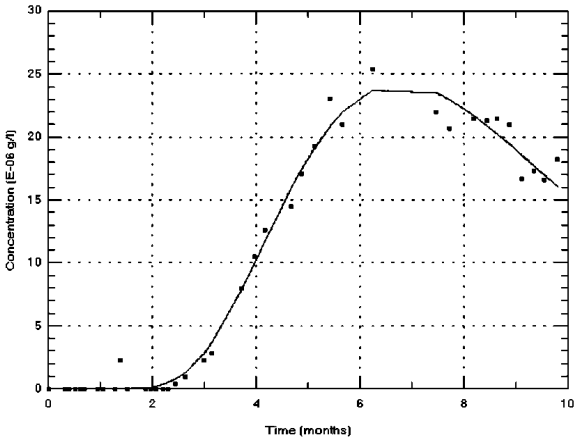

Figure 6. Observed and simulated 1,6-NDS tracer recovery in well MG-30D.

The results of the interpretation as shown in Fig. 6 and Table 3 indicate that the only one flow channel was required for each well pair. The most affected well is MG-30D with a tracer recovery of 0.0677. The total tracer mass recovery is 0.1897 or 114 kg out of the 600 kg injected. The principal conduit of these east-moving fluids is the Mamban Fault, which later traverses along the Ewex Fault.

The 2,6 NDS tracer injected in MG-5RD that would duplicate injected fluids from MG-RD1B pad established a connection between MG-5RD and the wells located south of the production field (MG-7D, MG-16D, MG-2D, MG-22D, MG-23D). These fluids recorded the highest tracer mass recovery of 0.2548, or 153 kg of the 600 kg of the tracer injected among the three tracers injected, with well MG-16D and MG-7D being the most affected at 0.0804 and 0.0778, respectively (Table 4). These fluids travel at moderately fast speeds with arrival times ranging from 20 to 56 days or a mean velocity of 215 to 600 m/month. A single path model gives a best fit for most well pairs as for MG-16D as shown in Fig. 7. The tracer/brine possibly follows the trace of the highly permeable Catmon Fault, which the injection wells intersected, and traverses through the Mahanagdong Fault to reach the southern production wells. Tracers were first observed in MG-16D and MG-7D that intersected the Mahanagdong Fault at moderate depths, followed by MG-2D and MG-22D, which intersected the structure near each wells' bottom.

Table 4. Model parameters used to simulate 2,6-NDS recovery of wells from MG-5RD.

Well	Channel length, x (m)	u (m/s)	Aϕ (m^2)	αL (m)	Mi/M (kg/kg)
MG7D	2100	0.00024	15.72	166	0.0548
	2200	0.00010	16.07	85	0.023
MG16D	1650	0.00016	34.55	327	0.0804
MG2D	1050	0.000083	27.86	150	0.033
MG22D	1800	0.00011	30.14	259	0.0464
MG23D	2400	0.00011	11.33	324	0.0172

In general, the tracer return data indicate that the injected waters travel throughout the area by two modes: first by direct, small volume flow paths, such as along fractures as in the case of MG-21D, and secondly, by dispersion and mixing throughout the volume of reservoir, as displayed by fluids injected in MG-4DA and MG-5RD.

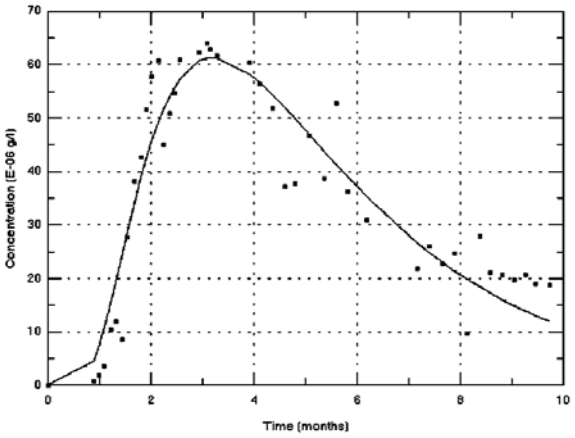

Figure 7. Observed and simulated 2,6-NDS tracer recovery in well MG-16D.

However, it is observed that in all of the positive responding wells, only a relatively small percentage of tracers are recovered, with a minimum of 0.27% in MG-28D (1,5 NDS) to a maximum of 8% in MG-16D (2,6 NDS). Most of the tracers, therefore, appear to disperse and diffuse throughout the reservoir volume. In the case of MG-21D, as with the other affected wells, although the recovery profiles indicated fast and almost direct connections, only a fraction of the tracers travel through the flow-channels.

The tracer results are generally consistent with the interpretation from geochemical monitoring. Wells MG-3D, MG-14D, MG-28D, MG-30D and MG-31D showed elevated levels of Cl_{RES} concentrations, coupled with stable or reduced TQtz and CO_{2TD} levels indicating the influx of injection returns.

The 1,6 NDS tracer results confirmed the hydrological connection between MG-4DA and the MG-DL wells. The tracer test conducted last October 1999 using ^{125}I tracer with MG-4DA as the injector well showed six positive-responding wells (MG-26D, 27D, 29D, 30D, 31D) all located in the MG-DL pad in MG-B sector. The preferential migration of the fluids towards this area was influenced by the large pressure draw down that has taken place in the MG-DL area (Delfin, et. al, year??).

The current tracer results likewise confirm the west flow preferential flow of fluids towards the northeast section of the field under the normal operating conditions of the production field. The tracer tests in October 1999 only indicated faster travel velocities of the fluids ranging from 357 to 462 m/month and slightly higher tracer recovery at 2.17 to 11%.

The 2,6 NDS tracer results similarly confirmed the connection between MGRD1 injection sink and the production wells at the south section of the Mahanagdong field. Inflow of injection returns from MGRD1B pad to these wells have been observed since 2000 up to the present based on their uniform increases in Cl_{RES} concentrations and decline in its CO_{2TD} but relatively stable TQtz values. The long distance (~2.0 kms) between the injection sink and the production sector enables the brine to be reheated before reaching the production sector thereby reflecting the stable TQtz temperatures of the wells.

4.2 Cooling Predictions

The data in Tables 2 to 4, which are the principal results of the analysis of the different tracer test data, were used as basis for the cooling predictions. As earlier stated, the flow-channel thickness and height are assumed to be equal, simulating a small surface area, pipe-like flow with high porosity, resulting to rapid cooling. Calculations assumed two porosity values of 6% and 11%, which are the minimum and maximum measured porosity in the Mahanagdong field. The cooling prediction results are shown in Tables 5 to 7.

Table 5. Cooling predictions for 1,5- NDS affected wells.

Well	Predicted temp decline °C (months)		Actual temp decline °C
	ϕ = 6%	ϕ = 11%	
MG3D	2.5° (80)	2.5° (50)	20° (25)
MG14D	0.5° (96)	0.5° (65)	25° (14)
MG28D	5° (60)	5° (50)	10° (12)
MG31D	0.3° (100)	0.4° (75)	6° (36)

Table 6. Cooling predictions for 1,6-NDS affected wells.

Well	Predicted temp decline °C (months)		Actual temp decline °C
	ϕ = 6%	ϕ = 11%	
MG29D	0° (100)	0.2° (100)	2° (60)
MG3D	0° (100)	0° (100)	46° (25)
MG27D	0° (100)	0.1° (100)	14° (66)
MG30D	0° (100)	0.2° (100)	10° (22)
MG31D	0° (100)	0° (100)	6° (36)
MG14D	0° (100)	0° (100)	25° (14)

Table 7. Cooling predictions for 2,6-NDS affected wells.

Well	Predicted temp decline °C (months)		Actual temp decline °C
	ϕ = 6%	ϕ = 11%	
MG7D	3° (100)	4° (70)	3° (72)
MG16D	8° (100)	9° (70)	0°
MG2D	1.5° (90)	2° (60)	7° (57)
MG22D	1° (100)	2° (100)	0°
MG23D	0°	0.2° (100)	11°

The results of the predictions indicate that the temperature of the water pumped from well MG-3D will decline by 2.5°C in 4 to 7 years, in MG-14D by 0.5°C in 5 to 8 years, in MG-28D by 1°C in 4 to 5 years and in MG-31D by 0.3°C to 0.4°C in 6 to 8 years due to the inflowing brine from the north.

For the fluids from the west, predictions indicate that it would have no significant cooling effect in MG-3D, MG-14D and the MG-DL wells within the next 8 years.

For wells in the south, predictions indicate that the temperature of the water in MG-7D will decline by 3°C to 4°C in 6 to 8 years, the water in MG-16D will decline by 8 to 9°C in 6-8 years and the water in MG-2D will decline by 1.5 to 2°C in 5 to 8 years. Meanwhile, it is predicted that the waters in MG-22D will decrease by 1 to 2°C in 8 years while MG-23D will not experience significant cooling of the fluids.

In general, the tracer results indicate that if the current injection load is maintained in Mahanagdong, no significant

thermal breakthrough is foreseen to occur among the production wells in the next 8 years. There seems to be no significant effect on the magnitude of temperature decline even after if the value of rock porosity is varied.

A comparison of the predicted temperature decline with the measured temperature decline from TQtz geothermometer of the fluids from each well was attempted to test the accuracy of the predictions. Results as shown in Tables 5 to 7 generally show higher actual temperature declines than the predicted cooling. Well MG-3D for example, displayed a temperature decline of 20°C against the predicted temperature decline of 2.5°C when the well was affected by injection returns. The other wells, MG-30D and MG-31D manifested a 10°C and 6°C drop, respectively, against the predicted decline of 0.2°C and 0°C.

It is possible that the true changes in temperature of the production wells in Mahanagdong mainly due to injection have been masked by the combination of other processes. It should be noted that prior to the period of rapid temperature decline in MG-3D, MG-14D and MG-28D and MG-31D, continuous condensate injection at 70 to 90 kg/s was done in the adjacent acid well MG-9D. Moreover, no recent downhole surveys have been conducted to verify if these wells are free from blockages. All these factors may have significant contributions on the final temperature of the wells.

It should be also noted that the injected water that travel through diffusion and dispersion may cool the production well to some degree, although cooling due to this mode of transport cannot be predicted with any accuracy.

Finally, there is no unique solution to the analysis of the tracer results. The data set can be simulated using more than one model for comparison and validation. Other models consider mechanical dispersion and retardation of the tracers by diffusion into the rock matrix that will significantly affect the tracer return curve.

5.0 CONCLUSIONS

The results of the three NDS tracer tests confirm the hydrological connection between the injection and production wells.

Fluids from the north travel at fast velocities, implying an almost direct flow-path to the production wells while fluids from the west and south travel at slower rates, undergoing mixing and dispersion throughout the volume of the reservoir.

The tracer results indicate that with the current injection load in the Mahanagdong production field, no significant cooling is expected to happen among the Mahanagdong production field in the next 8 years.

The discrepancy in the cooling predictions may be due to the masking effect of the other processes concurrent with the inflow of injection returns in the wells.

The NDS tracer test data can be simulated using other numerical models to further refine the interpretation.

6.0 REFERENCES

Arason, I.: TRMASS. A program to integrate observed data and give total recovered mass of tracer. (1993) Orkustofnun.

Arason, I.: TRINV . Tracer Inversion program. (1993) Orkustofnun.

Axelsson, G., Bjornsson, G., and Arason, I.: TRCOOL: A program to calculate cooling of production water due to injection of cooler water to a nearby well. (1993). Orkustofnun.

Axelsson, G., Flovenz, O.G., Hauksdottir, S., Hjartarson, and A., Lui, J.: Analysis of tracer test data, and injection-induced cooling, in Laugaland geothermal field, N-Iceland, *Geothermics*, vol. 30 (2001), pp. 697-725.

Axelsson, G., et al., (1994). Injection experiments in low temperature geothermal areas in Iceland. *Proceedings*, World Geothermal Congress, pp. 1991-1996.

Delfin, F.G., Barry, B., Dacillo, D.B., and Marcelo, E.A.: Analysis and Interpretation of ^{125}I Tracer Test Results, Mahanagdong Geothermal Reservoir, Leyte, Philippines. Paper presented at IAEA RAS/8/092 and NT/0/060 Coordination Meeting on Isotopic and Geochemical Techniques in Geothermal Exploration and Reservoir Management (2001).

Molina, P.O., Tanaka, T., Itoi, R., Siega, F.L., and Ogena, M.S.: Analysis and Interpretation of NDS Tracer Test Results at the Mahanagdong Geothermal Field, Philippines. Proceedings, 25th Annual PNOC-EDC Geothermal Conference (2004). Pp. 171-179.

Nogara, J, B., and Sambrano, Ma.G.: Tracer Tests Using Naphthalene Di-Sulphonates in Mindanao Geothermal Production Field, Philippines. Proceedings, 25th Annual PNOC-EDC Geothermal Conference (2004). pp. 131-137.

Rose, P.E., Johnson, S.D., and Kilbourn, P.M.: The Application of the Polyaromatic Sulfonates as Tracers in Geothermal Reservoirs, Goethermics, vol. 30 (2001), pp. 617-640.

Rose, P.E., Johnson, S.D., Kilbourn, P.M., and Kasteler, C.: Tracer Testing t Dixie Valley, Nevada using 1-Naphthalene Sulfonate and 2,6-Naphthalene Disulfonate. Proceedings, 26th Workshop on Geothermal Reservoir Engineering. Stanford, University. Stanford, CA (2002).

Salonga, N. D., Dacillo, D. B., and Siega, F. L.: Providing solutions to the rapid changes induced by stressed production in Mahanagdong geothermal field, Philippines, *Geothermics*, vol. 33 (2004), pp. 181-212.